

Improvement of corrosion resistance of transparent conductive multilayer coating consisting of silver layers and transparent metal oxide layers

Katsuhiko Koike, Fumiharu Yamazaki, Tomoyuki Okamura, and Shin Fukuda

Citation: *J. Vac. Sci. Technol. A* **25**, 527 (2007); doi: 10.1116/1.2722758

View online: <http://dx.doi.org/10.1116/1.2722758>

View Table of Contents: <http://avspublications.org/resource/1/JVTAD6/v25/i3>

Published by the AVS: Science & Technology of Materials, Interfaces, and Processing

Related Articles

In situ fabrication of blue ceramic coatings on wrought Al Alloy 2024 by plasma electrolytic oxidation
J. Vac. Sci. Technol. A **30**, 021302 (2012)

Influence of substrate temperature and bias voltage on properties of chromium nitride thin films deposited by cylindrical cathodic arc deposition
J. Vac. Sci. Technol. A **29**, 051515 (2011)

Ultrathin TiSiN overcoat protection layer for magnetic media
J. Vac. Sci. Technol. A **29**, 051502 (2011)

High-corrosion-resistant Al₂O₃ passivation-film formation by selective oxidation on austenitic stainless steel containing Al
J. Vac. Sci. Technol. A **29**, 021002 (2011)

Low-energy ion bombardment to tailor the interfacial and mechanical properties of polycrystalline 3C-silicon carbide
J. Vac. Sci. Technol. A **28**, 1259 (2010)

Additional information on *J. Vac. Sci. Technol. A*

Journal Homepage: <http://avspublications.org/jvsta>

Journal Information: http://avspublications.org/jvsta/about/about_the_journal

Top downloads: http://avspublications.org/jvsta/top_20_most_downloaded

Information for Authors: http://avspublications.org/jvsta/authors/information_for_contributors

ADVERTISEMENT



K-Alpha XPS System
Maximize productivity.

[Learn more >](#)

Thermo
SCIENTIFIC

Improvement of corrosion resistance of transparent conductive multilayer coating consisting of silver layers and transparent metal oxide layers

Katsuhiko Koike,^{a)} Fumiharu Yamazaki, Tomoyuki Okamura, and Shin Fukuda
Mitsui Chemicals, Inc., Sodegaura, Chiba 299-0265, Japan

(Received 16 September 2005; accepted 13 March 2006; published 12 April 2007)

An optical filter for plasma display panel (PDP) requires an electromagnetic shield with very high ability. The authors investigated a transparent conductive multilayer coating consisting of silver (Ag) layers and transparent metal oxide layers. The durability of the multilayer sputter coating, including the silver layer, is very sensitive to the surrounding atmosphere. For example, after an exposure test they found discolored points on the multilayer sputter coatings, possibly caused by migration of silver atoms in the silver layers. In their investigation, they modified the top surface of the multilayer sputter coatings with transition metals to improve the corrosion resistance of the multilayer coating. Specifically, they deposited transition metals 0.5–2 nm thick on the top surface of the multilayer coatings by sputtering. They chose indium tin oxide (ITO) as the transparent metal oxide. They applied the multilayer sputter coatings of seven layers to a polyethylene terephthalate (PET) film substrate. A cross-sectional structure of the film with the multilayer coatings is PET film/ITO/Ag/ITO/Ag/ITO/Ag/ITO. They evaluated the corrosion resistance of the films by a salt-water immersion test. In the test, they immersed the film with multilayer coatings into salt water, and then evaluated the appearance, transmittance, and electrical resistance of the multilayer coatings. They investigated several transition metals as the modifying material, and found that titanium and tantalum drastically improved the resistance of the multilayer coatings to the salt-water exposure without a significant decline in transmittance. They also investigated the relation between elapsed time after deposition of the modifying materials and resistance to the salt water. Furthermore, they investigated the effects of a heat treatment and an oxide plasma treatment on resistance to the salt water. © 2007 American Vacuum Society. [DOI: 10.1116/1.2722758]

I. INTRODUCTION

We use transparent conductive films for many applications, such as electromagnetic shields and transparent electrodes for liquid crystal display, plasma display panel (PDP), and electroluminescent display. We have conventionally applied transparent conductive oxides such as indium tin oxide (ITO) for the transparent conductive film. Lower electric resistance is required for the transparent conductive film to achieve a low-power-consumption display and high electromagnetic shielding. An optical filter for PDP requires the electromagnetic shield to have very high shielding capability. We have applied¹ transparent conductive multilayer coatings consisting of silver (Ag) layers and transparent metal oxide layers.²

The multilayer sputter coatings with the silver layer are very sensitive to the surrounding atmosphere.^{3–5} For example, when the coatings are exposed to the atmosphere, we found discolored spots on the multilayer sputter coatings, possibly caused by the migration of silver atoms in the silver layers.

Silver atoms aggregate around the presence of halogen atoms. Chlorine is a typically present in the ambient atmosphere and is well known that it deteriorates Ag based film. It

is easy to imagine that chlorine in the surrounding atmosphere causes the discolored spots on the multilayer sputter coatings.

Figure 1 shows a schematic of the proposed process. Firstly, the chlorine ion (Cl^-) attacks the surface of the multilayer sputter coating. Chlorine (Cl) atoms pass through the ITO layer, and then reach the silver layer. Finally, the silver atoms aggregate around the chlorine atoms and form a cluster. Some of the clusters grow and can be seen by the naked eye.

Preventing Cl^- from invading the multilayer sputter coating is a strong candidate process for improving the corrosion resistance of the transparent conductive multilayer. In this study, we deposited a transition metal on the top surface of the multilayer coatings by sputtering.

II. EXPERIMENT

A. Sample preparation

We prepared a film with multilayer sputter coatings of nine layers and the top barrier layer was deposited from the transition metal. The multilayer sputter coating consists of silver (Ag) layers and ITO layers. Figure 2 shows a cross-sectional structure of the film with multilayer sputter coatings and the top barrier layer deposited from the transition metal. The cross-sectional structure is a PET film/ITO(36 nm)/Ag(9 nm)/ITO(77 nm)/Ag(13 nm)/ITO(80 nm)/Ag(12 nm)/ITO(86 nm)/Ag(12 nm)/ITO(48 nm)/

^{a)}Electronic mail: katsuhiko.koike@mitsui-chem.co.jp

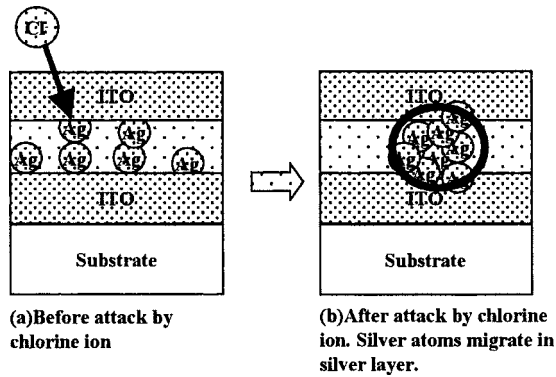


FIG. 1. Schematic of cross-sectional view of multilayer sputter coatings, showing silver migration process that is activated by response to chlorine ion.

top barrier layer deposited from the transition metal (1.2 nm). We deposited each layer on a polyethylene terephthalate (PET) film substrate by dc magnetron sputtering. Table I shows the transition metals we used for the top barrier layer. We used Ti, Zr, Hf from the 4th group; V, Nb, Ta from the 5th group; Mo, W from the 6th group; Mn from the 7th group; Ni from the 10th group and; and Cu from the 11th group of the Periodic Table. The reaction gas was a mixed gas of argon (Ar) and oxygen (O_2) for ITO deposition, and was pure argon (Ar) gas for silver and the top barrier layer from the transition metal.

B. Sample analysis

We evaluated the optical and electric properties of the multilayer sputter coatings with the top barrier layer deposited from Ti. We measured the transmittance of the sample by a spectrometer with an integrating sphere. We measured the sheet resistance of the sample by a four-terminal resistivity meter.

We investigated the elemental composition of the surface of the multilayer sputter coatings with the top barrier layer deposited from Ti by x-ray photoelectron spectroscopy (XPS). The instrument was an ESCAB 220i XL. The source of the x ray was $Mg K\alpha$. The degree of vacuum was 2×10^{-7} Pa. The resolution of the binding energy was 1 eV. A

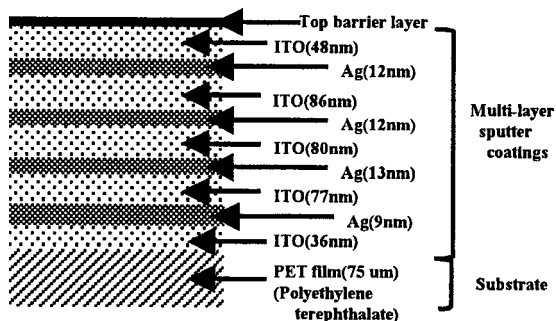


FIG. 2. Cross-sectional view of PET film with multilayer sputter coatings for PDP filter. Top barrier layer is deposited from transition metal target. Thickness of the top layer measured by x-ray fluorescence thickness meter is 1.2 nm.

TABLE I. Transition metals in the Periodic Table used in this study as a top barrier layer.

	4th	5th	6th	7th	10th	11th
4	Ti	V		Mn	Ni	Cu
5	Zr	Nb	Mo			
6	Hf	Ta	W			

survey scan was made to determine the binding energies. We evaluated the thickness of the top barrier layer deposited from Ti by x-ray fluorescence thickness meter.

C. Salt-water immersion test

We applied a salt-water immersion test to evaluate the resistance of the multilayer sputter coatings to chlorine ion. Figure 3 shows a schematic of the salt-water immersion test that we applied. We laminated the film with the multilayer coatings on a 3-mm-thick plastic sheet. Dimensions of the sample were $50 \times 50 \text{ mm}^2$. We immersed the sample in 0.1 mol/l of salt water for 17 h. The aggregation of Ag which occurs to the sample which was exposed to the atmosphere is caused by the chlorine ion which the atmospheric hygroscopic-moisture ionized. The salt-water immersion test is the practical technique that it is possible to supply Cl^- while controlling the number of the ions.

D. Aging

We aged the film with multilayer sputter coating using the top barrier layer deposited from Ti, expecting that corrosion resistance of the multilayer sputter coating would improve. We exposed the film to the atmosphere at room temperature for five days. Then, we evaluated the corrosion resistance of the film with multilayer sputter coating by the salt-water immersion test.

E. Annealing

We also annealed the film with multilayer sputter coating using the top barrier layer deposited from Ti at 60°C for 17 h, expecting that the corrosion resistance of the multilayer sputter coating would improve. We used two surrounding environments for the annealing process: the atmosphere in a

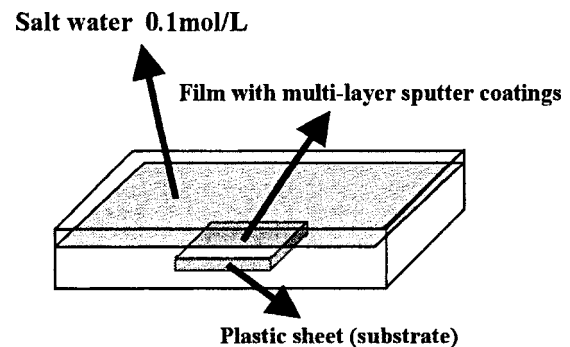


FIG. 3. Schematic illustration of salt-water immersion test.

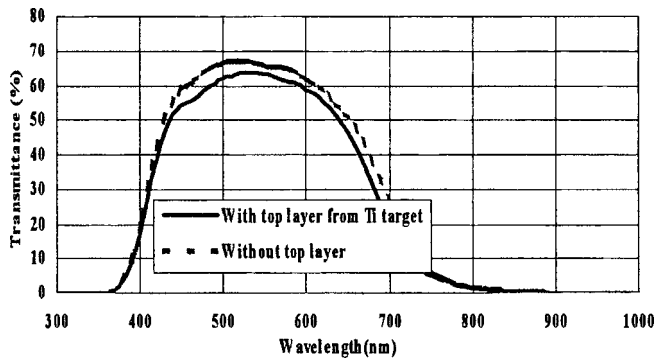


FIG. 4. Transmittance spectra of films with multilayer sputter coatings. Transmittance drop of 2.9% at 550 nm by top layer is acceptable.

drying oven, and vacuum in a drying oven. We also evaluated the corrosion resistance of the films with multilayer sputter coating by the salt-water immersion test.

III. RESULT AND DISCUSSION

A. Feature of sample with top barrier layer from Ti metal target

Figure 4 shows the transmission spectrum of the film with multilayer sputter coating with the top barrier layer from the Ti metal target. The reference transmission spectrum of the multilayer sputter coating without the top barrier layer is also shown in Fig. 4. Transmittance of the multilayer sputter coating using the top barrier layer from Ti was lower by 2.9% at 550 nm compared to the reference. This transmittance drop of 2.9% is still acceptable for optical filters. In addition, we confirmed that the transmittance of the multilayer sputter coating increased just after deposition of the top barrier layer from Ti, and was close to the transmittance of the multilayer without the top barrier layer possibly because of oxidation of the top barrier layer from the Ti metal target. We therefore concluded that the top barrier layer deposited from Ti would not lower the transmittance of the multilayer sputter coating.

Table II shows the sheet resistance of the film with multilayer sputter coating using the top barrier layer from the Ti metal target. As a reference, the sheet resistance of the film with multilayer coating without the top barrier layer is shown in the lower column in Table II. The sheet resistance was the same, 1.1 Ω /sq, in both samples. Figure 5 shows the elemental composition of the surface of the film with multilayer sputter coating using the top barrier layer from the Ti metal target measured by XPS. We confirmed Ti 2p peaks at 458.7 eV.

From the result of x-ray photoelectron spectroscopy shown in Fig. 5. We think that the final state of Ti is very near TiO_2 . But, when thinking of Ti top barrier layer thick-

TABLE II. Sheet resistance of films with multilayer sputter coatings. After deposition of the top layer, high conductivity is still maintained.

With top layer from Ti target (Ω /sq)	1.1
No top layer (Ω /sq)	1.1

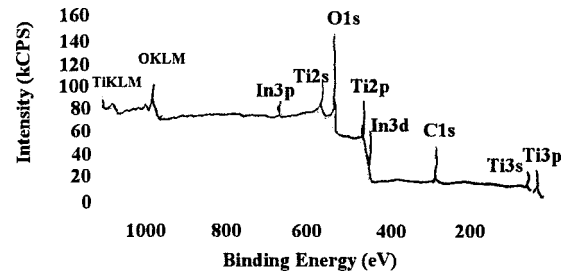


FIG. 5. Elemental composition of surface measured by XPS. Ti2p peak at 458.7 eV is observed.

ness being 1.2 nm which are equivalent about 1 only for the atomic layer, we think that the atomic density of Ti is not enough to form the structure of general TiO_2 which is represented by rutile or anatase.

B. Corrosion resistance of film with top barrier layer deposited from transition metal targets

Figure 6 shows the samples after exposure to the salt-water immersion test by 0.01 mol/l salt water for 17 h. The multilayer sputter coatings with the top barrier layer deposited from Ti, Ta, Nb did not change and maintained their transparency. There was a slight change for W, including a slight loss of transparency. For Mn, the sample lost its trans-

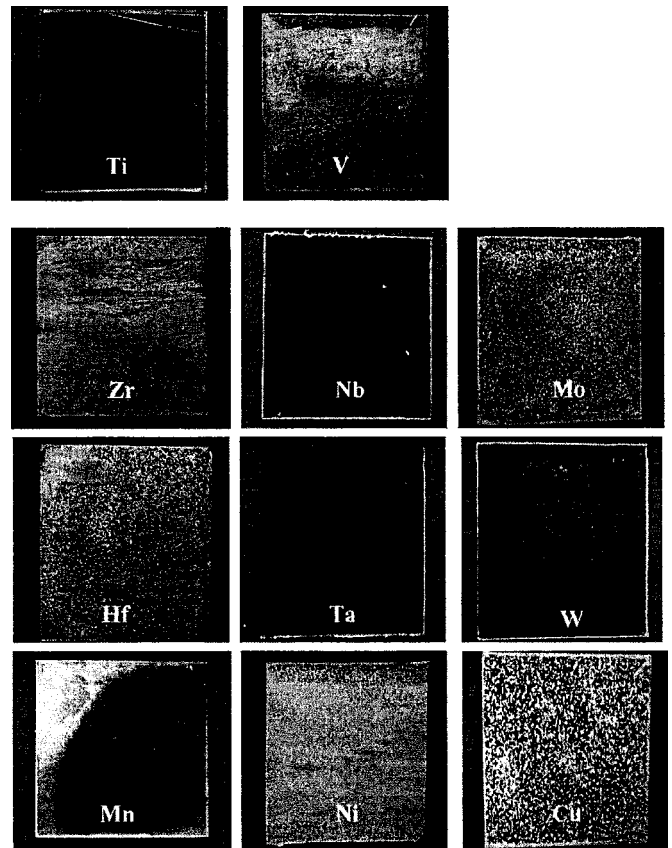


FIG. 6. Samples after the salt-water immersion test. Concentration of salt water is 0.01 mol/l. Test time is 17 h.

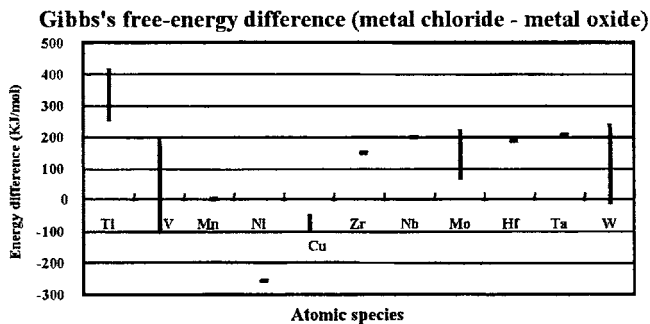


FIG. 7. Gibbs's free-energy difference (kJ/mol) between metal chloride-metal oxide. Transition metals with higher Gibbs's free-energy difference would lead to higher corrosion resistance.

parency only along the perimeter of the sample. The multilayer coating with the top barrier layer deposited by Ni, Cu, Zr, Hf, V, Mo, Pd became opaque.

We concluded that the ability of Ti, Ta, Nb to improve the corrosion resistance of the multilayer sputter coating was highest in the materials we evaluated. W follows these Mn, Ni, Cu, Zr, Hf, V, and Mo do not show any ability for improving the corrosion resistance of the multilayer sputter coatings. We summarized the order of the ability for improving the corrosion resistance of the multilayer sputter coating as Ta, Nb, Ti > W > Mn, V, Zr, Mo, Cu, Hf, Ni.

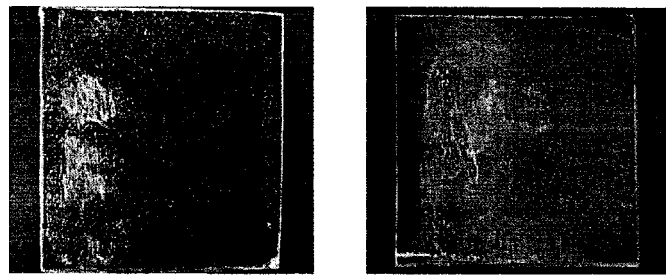
As well known, Cl^- is the trigger leading to the aggregation of Ag. We can guess that major product of the corrosion is Ag, and AgCl is not the main ingredient.

C. Gibbs's free-energy study

We ranked the ability for improving the corrosion resistance of multilayer sputter coating by applying Gibbs's free-energy difference between metal chloride and each transition metal. The surface of the transition metals exposed to atmosphere is oxidized at varying degrees and becomes more stable. In our study, the transition metal atoms on the multilayer sputter coatings would oxidize easily just after exposure for the following two reasons. First, metal oxide is in a lower energy state than a metal. Second, the transition metal atoms can contact with oxide atoms, because the 1.2-mm-thick layer of the transition metal atoms is located as an island structure. We considered that transition metals with a high Gibbs's free-energy difference between metal chloride and metal oxides would provide a possible material for high corrosion resistance.

Meanwhile, rates of oxidation differ among transition metal. In the salt-water chloride ion approach to metal oxide, the chlorine ion is exchanged for an oxide atom of the metal oxide when metal chloride is more stable than metal oxide. Then, the chlorine atom can reach the silver layer, and causes a migration of silver atoms. We think that transition metal layer with high Gibbs's free energy difference between metal chloride and metal oxide works as a transparent ion barrier layer.

Based on the two assumptions—that (1) there is a high Gibbs's free-energy difference between metal chloride and metal oxides, and (2) high reactivity with oxide—the trans-



(a) Aged in atmosphere for 5 days

(b) No aging

FIG. 8. Aged samples after the salt-water immersion test. Concentration of salt water is 0.1 mol/l and test time is 17 h. The corrosion resistance increased with time.

parent conductive multilayer coating layers will show high corrosion resistance. Figure 7 shows the Gibbs's free-energy difference between the metal oxide and metal chloride for each transition metal we applied to the top barrier layer. Transition metal oxides have several possible structures. The dots in Fig. 7 show the Gibbs's free-energy⁶ difference for the most feasible structure after deposition. The bars show the range of the Gibbs's free-energy difference for possible structure. Focusing on the dots for each transition metal, Ti, Zr, Hf, Nb, and Ta lead to a relatively large Gibbs's free-energy difference. The energy difference is more than 150 kJ/mol for these transition metals.

Ni, Cu, and Mn lead to a small Gibbs's free-energy difference, and therefore these transition metals lead to less corrosion resistance. These transition metals can be easily attacked by chloride ions.

Titanium (Ti) has a high reactivity with oxygen^{7,8} and forms an oxide layer, even in an ultrahigh vacuum environment. Therefore, we think that Ti oxidized just after exposure to the atmosphere and becomes stable in our study. Ti with a high corrosion resistance shown by the salt-water immersion test satisfies two of the requirements for the high corrosion resistance.

Ta, Nb lead to high corrosion resistance, as shown in Fig. 6. In Fig. 7, we confirmed that Ta, Nb have a high Gibbs' free-energy difference between the metal oxide and metal chloride. We predict that Ta and Nb have a high reactivity with oxygen like Ti demonstrates.

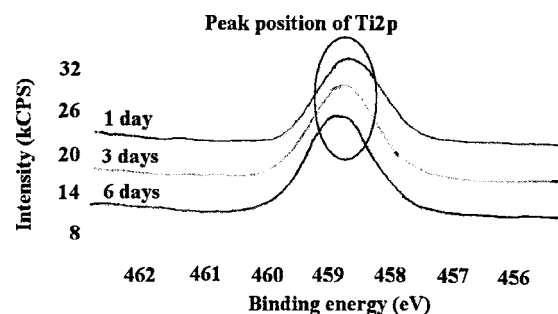


FIG. 9. Elemental composition analysis by XPS. Analysis of $\text{Ti}2p$ peak energy during aging process. Peak from $\text{Ti}2p$ shifts to higher energy direction. Ti shifts to higher oxide state with time.

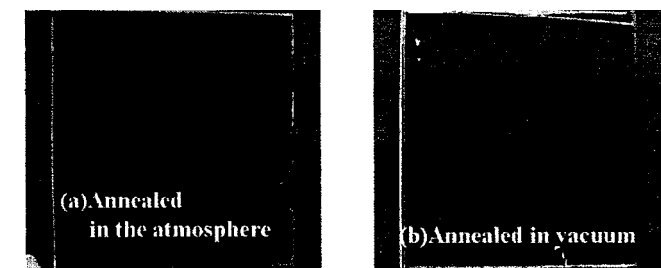


FIG. 10. Annealed samples after the salt-water immersion test. Temperature for annealing is 60 °C. Time for annealing is 17 h. Concentration of salt water is 0.1 mol/l. Test time is 17 h.

We observed low corrosion resistance led by Zr, despite a high Gibbs's free-energy difference between metal chloride and metal oxide for Zr. Oxidation of Zr thin film progresses slower at room temperature.⁹ We think that Zr had not oxidized sufficiently on the salt immersion test, in contrast to the Ti case; therefore Zr possesses lower corrosion resistance to the salt-water immersion test. V, W, Mo could be oxidized and were in a low energy state. Figure 7 shows these metals exhibited a high Gibbs's free-energy difference between metal chloride and metal oxide. We predict that the oxidation rate for V, W, Mo is low from the result of the salt-water immersion test, and these metals are in a relatively higher energy oxide state just after exposure to the atmosphere.

D. Aging effect and annealing effect for the multilayer with top barrier layer deposited from Ti

Figure 8(a) shows the aged sample after the salt-water immersion test for 17 h by 0.1 mol/l salt water. Colored spots are visible on the sample. However, the sample still maintains its transparency after the salt-water immersion test. In Fig. 8(b), the sample without aging lost its transparency after the salt-water test. Thus, we conclude that the corrosion resistance of the multilayer sputter coating with the top barrier layer deposited from Ti was improved by the aging process. Figure 9 shows a shift of the Ti2*p* peak by XPS analysis with time during the aging process. We found that the peak position shifted in a higher binding-energy direction. This suggests that Ti shifts to a higher oxide state with time. In addition, Figures 10(a) and 10(b) show the appearance of the annealed samples after the salt-water immersion test for 17 h by 0.1 mol/l salt water. The sample in Fig. 10(a) was annealed in the atmosphere at 60 °C, and the sample in Fig. 10(b) was annealed in vacuum at 60 °C. Comparing these with Fig. 8(a), we conclude that the annealing accelerates the aging process.

E. Gibbs's free-energy study for aging and annealing effect

We considered the aging and annealing effect, applying Gibbs's free-energy difference between metal chloride and metal oxide. Titanium oxide shows several possible formations such as TiO, TiO₂ (anatase, rutile), Ti₂O₃, and Ti₃O₅.

TABLE III. Gibbs's free-energy difference of Ti compound (metal chloride-metal oxide) (kJ/mol). Change of Gibbs's free-energy difference to higher direction by aging would lead to higher corrosion resistance.

Ti ₂ O ₃	Ti ₃ O ₅	TiO ₂
253	308	420

Gibbs's free energies⁶ are -495.0 kJ/mol for TiO, -884.5 kJ/mol for TiO₂ (anatase), -889.5 kJ/mol for TiO₂ (rutile), -1434.2 kJ/mol for Ti₂O₃, and -2317.4 kJ/mol for Ti₃O₅. The surface of Ti oxides changes to TiO₂ just after exposure to the atmosphere because the surface of Ti is very reactive to oxide.¹⁰ However, for Ti film deposited on the multilayer sputter coatings, we predict different chemical reaction rates of oxidation from the surface of Ti, based on the result of the aging and annealing effect. We consider that the aging and annealing process changes the formation of titanium oxide to a more stable form. When calculating the Gibbs's free energies difference between metal chloride and metal oxide of each titanium oxide for 1 mol of Ti atom and arranging to be big in order, we lead an order of TiO₂, Ti₂O₃, TiO. This order is equivalent to the order of the ability for each titanium oxide to block chlorine. We could not identify the formation of titanium oxide. However, we expect the formation changes to be TiO first, Ti₂O₃ second, then TiO₂. In this process, the titanium oxide energy would decrease. The Gibbs's free-energy difference between titanium chloride and titanium oxide increases by decreasing the energy of titanium oxide (Table III). The aging or annealing effect improves the corrosion resistance by increasing the Gibbs's free-energy difference.

IV. CONCLUSION

In this study, we investigated several transition metals as the material for the top barrier layer of multilayer sputter coatings to improve the corrosion resistance. We found that titanium and tantalum drastically improved the resistance to salt water without a significant decrease in transmittance. In addition, we found that aging of the multilayer sputter coating with the Ti top barrier layer led to higher corrosion resistance, and annealing drastically accelerates the aging effect.

¹T. Okamura, S. Fukuda, K. Koike, H. Saigou, M. Yoshikai, M. Koyama, T. Misawa, and Y. Matsuzaki, *J. Vac. Sci. Technol. A* **19**, 1090 (2001).

²J. C. C. Fan, F. J. Bachner, G. H. Foley, and P. M. Zavracky, *Appl. Phys. Lett.* **25**, 693 (1974).

³K. Shimada, K. Koike, and S. Fukuda, *J. Vac. Soc. Jpn.* **46**, 214 (2003).

⁴S. J. Nadel, *J. Vac. Sci. Technol. A* **5**, 2709 (1987).

⁵Y. Aoshima, M. Miyazaki, K. Sato, Y. Akao, S. Takaki, and K. Adachi, *Jpn. J. Appl. Phys., Part 1* **40**, 4166 (2001).

⁶D. D. Wagman, W. H. Evans, V. B. Parker, R. H. Schumm, I. Halow, S. M. Bailey, K. L. Churney, and R. L. Nuttall, *J. Phys. Chem. Ref. Data* **11**, Suppl. 2 (1982).

⁷M. Kurahashi and Y. Yamauchi, *J. Vac. Sci. Technol. A* **17**, 1047 (1999).

⁸L. Q. Shi, Z. Y. Zhou, and G. Q. Zhao, *J. Vac. Sci. Technol. A* **18**, 2262 (2000).

⁹F. P. Fehlner, *J. Appl. Phys.* **38**, 2223 (1967).

¹⁰I. Vaquila, M. C. G. Passeggi, Jr., and J. Ferron, *Phys. Rev. B* **55**, 13925 (1997).